New latitude-based nannofossil zonations for the Campanian–Maastrichtian of the South Atlantic Ocean and their paleoceanographic implications

Rodrigo do Monte Guerra [a,*], Andrea Concheyro [b,c], Sherwood W. Wise Jr. [d], Sev Kender [e,f], Gerson Fauth [a]

[a] itt Fossil, Instituto Tecnológico de Micropaleontologia, Universidade do Vale do Rio dos Sinos (UNISINOS), Av. UNISINOS, 950, B. Cristo Rei/CEP: 93.022-000, São Leopoldo, RS, Brazil
[b] Instituto Antártico Argentino (IAA), Buenos Aires, Argentina
[c] IDEAN-CONICET, Departamento de Ciências Geológicas, Universidad de Buenos Aires, Pabellón II, Ciudad Universitaria, 1428 Buenos Aires, Argentina
[d] Department of Earth, Ocean and Atmospheric Sciences, Florida State University, Tallahassee, FL 32306-4100, USA
[e] Department of Geography, Centre for Environmental Geochemistry, University of Nottingham, University Park, Nottingham NG7 2RD, UK
[f] British Geological Survey, Keyworth, Nottingham NG12 5GG, UK

ARTICLE INFO

ABSTRACT

The global evolution of calcareous nannofossils during the Campanian–Maastrichtian interval is not fully understood, and nannofossil zonations for the central and South Atlantic Ocean are yet to be constructed. Here, we test the applicability of previous calcareous nannofossil zonations developed for other ocean basins, for biostratigraphy in the South Atlantic Ocean, and refine Campanian–Maastrichtian biostratigraphy in the region. We document calcareous nannofossil distributions at Deep Sea Drilling Project (DSDP) and Ocean Drilling Program (ODP) sites from the high, mid and low latitudes in the South Atlantic Ocean (DSDP Sites 354, 356, 511, 525A, and 530A, and ODP Sites 690C; 700B; 661A, and 1258A). Combining nannofossil occurrences with magnetostratigraphic schemes previously constructed for some of the sites, we propose three new zonations tied to the global magnetostratigraphic chrons, with distinct bio-horizons selected at different latitudinal regions. In this study we present detailed definitions of new South Atlantic Ocean Low-latitude (SAL), South Atlantic Mid-latitude (SAM) and South Atlantic High-latitude (SAH) zonations. We identified significant diachronism of some species between latitudes throughout the Campanian and Maastrichtian. These species diachronism, mainly between zonal markers from low and mid latitudes during the late Maastrichtian, was probably related to migration patterns due to fundamental paleoceanographic changes.

© 2016 Elsevier B.V. All rights reserved.

1. Introduction

The Late Cretaceous period records significant paleoceanographic and paleobiological changes related to surface-water temperatures and global climate (Jenkyns et al., 1994; Huber et al., 1995; Clarke and Jenkyns, 1999; Huber et al., 2002; Lees, 2002; Linnert et al., 2014). After the mid-Cretaceous (Albian–Turonian) hot greenhouse climate (e.g., Forster et al., 2007), bottom-water and sea-surface temperatures gradually declined throughout the latest Cretaceous (Coniacian–Campanian) before exhibiting several cooling and warming episodes in the Maastrichtian. The end of the Cretaceous culminated in a significant warming in the latest Maastrichtian (Li and Keller, 1998; Thibault et al., 2010; Friedrich et al., 2012; Thibault and Husson, 2016). These climate changes resulted in nannofossil migrations and provincialism,

which still needs to be fully documented (Thierstein, 1981; Thibault et al., 2010), and some of the highest diversities of calcareous nannofossils species from the Mesozoic to Recent (Bown et al., 1991).

The provinciality and diachronism of calcareous nannofossils pose a challenge for biostratigraphers, leading to unreliable stratigraphic interpretation and correlation. For instance, it has been noted by several authors that the global zonation of Burnett et al. (1998), encompassing three provinces termed Boreal, Tethyan/Intermediate and Austral, cannot be fully applied in several regions due to the absence and diachronism of some marker species (e.g., NW Australian margin, Howe et al., 2003; Campbell et al., 2004; NW Pacific, Lees and Bown, 2005; Equatorial Atlantic, Thibault and Gardin, 2006; Danish Basin, Sheldon, 2008). The Southern Ocean zonation of Watkins et al. (1996) also contains species that are different from those of the Austral scheme of Burnett et al. (1998). Moreover, both the Watkins et al. (1996) and the Burnett et al. (1998) zonations have yet to be tied to the standard magnetostratigraphic time scale so that the correlation of the bio-horizons among ocean basins should be achieved. In an isolated attempt to assess this issue, Thibault et al. (2010) documented the global

* Corresponding author.
E-mail addresses: rmguerra@unisinos.br (R. do Monte Guerra), andrea@gl.fcen.uba.ar (A. Concheyro), swise@fsu.edu (S.W. Wise), sev.kender@nottingham.ac.uk (S. Kender), gersonf@unisinos.br (G. Fauth).

diachronous first occurrence of *Micula murus* in the late Maastrichtian (moving from low to mid latitudes, see the Discussion section), and concluded that further work is needed to construct two distinct biozonations for the low- and mid-latitudes.

Biostratigraphic studies on Campanian and Maastrichtian calcareous nannofossils from the South Atlantic Ocean are limited to Deep Sea Drilling Project (DSDP) and Ocean Drilling Program (ODP) sites, mainly during the 1980s and 90s (Wise and Wind, 1977; Perch-Nielsen, 1977; Wise, 1983; Wind and Wise, 1983; Manivit, 1984; Manivit and Feinberg, 1984; Stradner and Steinmetz, 1984; Manivit, 1989; Pospichal and Wise, 1990; Crux, 1991; Erbacher et al., 2004). In addition to these studies, there are others on the Brazilian Continental Margin (Troelsen and Quadros, 1971; Freitas, 1984; Antunes, 1987; Gomide, 1989; Oliveira and Costa, 1997; Oliveira, 1997; Antunes, 1998; Guerra et al., 2010, 2012) and on the Antarctic Peninsula (Concheyro et al., 1991; Concheyro et al., 1994; Concheyro, 2004; Švábenická et al., 2012; Guerra et al., 2015). However, there is yet no assessment on the applicability of the previous zonations for the South Atlantic Ocean, as well as the degree of provincialism of marker species.

We revise Campanian and Maastrichtian calcareous nannofossil occurrences, taxonomy and biostratigraphy at selected DSDP and ODP sites in the South Atlantic Ocean (354; 356; 511; 525A; 530A; 661A; 690C; 700B and 1258A). Occurrences of marker species are tied to the paleomagnetic records where possible and we propose new separate zonations for the low-, mid- and high-latitudes and discuss their paleoceanographic significance.

2. Materials and methods

2.1. Site information

Our revised biostratigraphy is based on a quantitative analysis of nine DSDP and ODP sites from different locations of the South Atlantic Ocean (Fig. 1). Important information about each site (locality; water depth; stratigraphic range; main lithologies and number of samples studied) can be seen in Table 1.
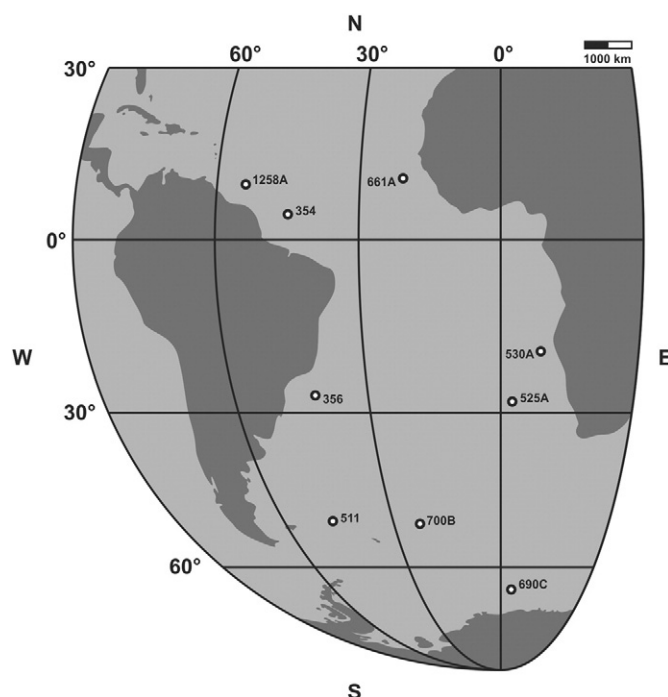

Fig. 1. Location map of sites selected for this study.

2.2. Sampling, preparation and analysis

One sample was taken per section of drillcore, corresponding to a sampling resolution of ~1.5 m. Samples were prepared following the standard smear-slide technique described in Bown and Young (1998).

A quantitative study was performed using a Zeiss Axio Imager A2 microscope at $1000\times$ magnification. At least 300 specimens were counted per sample, followed by the scanning of three more longitudinal traverses (~300 fields of view) for rare taxa missing in the initial counts, indicated in our range charts by "X". Sometimes, important markers were identified after the counting, denoting species present but do not represent only one specimen.

Preservation of calcareous nannofossils was evaluated under light microscope using qualitative criteria to assess the degree of etching and/or overgrowth, where "good" indicates specimens with little or no etching and/or overgrowth; "moderate" suggest that specimens exhibit moderate etching and/or overgrowth, but still easily recognizable; and "poor" shows specimens with extreme etching and/or overgrowth (Roth and Thierstein, 1972; Roth, 1983).

Although the original taxonomic and biostratigraphical results are available on DSDP and ODP websites, we re-examined 520 samples in order to apply up-to-date taxonomic and biostratigraphic concepts, since most studies were conducted several decades ago. The range charts for each site selected for this study are available as supplementary data Tables S1 to S9, where it is possible to visualize the nannofossil occurrences, preservation and abundances, as well as the biostratigraphic interpretations.

2.3. Taxonomy

The taxonomic identification is based on Perch-Nielsen (1985); Burnett et al. (1998), original descriptions and Nannotax3 (Young et al., n.d. - website that provides important information regarding calcareous nannofossil taxonomy, URL: http://ina.tmsoc.org/Nannotax3). We recognized 195 species, also in poorly preserved samples, which are all listed in Appendix 1 (available as Supplementary data) with the ones relevant for biostratigraphic interpretations illustrated in Fig. 2. Some Cretaceous species older than Campanian–Maastrichtian were recognized during the taxonomic analysis, being considered as reworked (e.g., *Braarudosphaera africana*, *Flabellites oblongus*, *Eprolithus eptapetalus*, *Lithastrinus septenarius*, *Nannoconus* sp. and *Assipetra* sp. on Site 530A; *Assipetra* sp. and *Rhagodiscus asper* on Site 356; and *Eprolithus floralis* on Site 661A).

2.4. Biostratigraphic zonations

In order to construct biozonations applicable to the South Atlantic Ocean, we analyzed the position of the first and last occurrences (FO and LO, respectively) of the species within the studied sites. Clear compositional differences were observed at the high-latitude DSDP/ODP Sites 511, 690B, and 700B, when compared to the other locations, confirming the well-known provincialism of the Southern Ocean (Watkins et al., 1996). Mid-latitude Sites 356, 525A and 530A contain similar flora to low-latitude Sites 354, 661A, and 1258A, although it became apparent after analysis of the sequence of bio-horizons and chronostratigraphic comparison that there were significant differences in the timing of the bio-horizons between these regions. We, therefore, propose two further provinces for the low and mid latitudes, based on the sequence of bio-horizons recorded between sites.

We defined bio-horizons for our zonations based on the following criteria: (a) that they occur in the majority of the sites within a given province; (b) that the order of the bio-horizons is consistent among provinces; (c) that each bio-horizon can be correlated to a magnetostratigraphic chronozone; and (d) that the bio-horizons occur in the same chronozone (where this information is available) or so

Table 1
Relevant information about each site studied herein (locality; water depth; stratigraphic range; main lithologies and number of samples studied).

Site	Year	Coordinates	Locality	Water depth (m)	Stratigraphic range	Main lithologies	Number of samples	Magnetostratigraphy	Figure
354	1974	05°53.95′S 44°11.78′W	Ceará Rise	4052	Early?/Late Maastrichtian	Marly nannofossil chalk, and calcareous chalk	9	No data	5
356	1974	28°17.22′S 45°05.28′W	Sao Paulo Plateau	3175	Middle/Late Campanian to Late Maastrichtian	Foraminiferal-nannofossil chalk, nannofossil chalk, and marly calcareous chalk	39	No data	8
511	1980	51°00.28′S 46°58.30′W	Falkland Plateau	2589	Early to Late Campanian	Calcareous ooze, zeolitic calcareous foraminiferal ooze, zeolitic claystone, and claystone	81	No data	11
525A	1980	29°04.24′S 02°59.12′E	Walvis Ridge	2467	Late Campanian to Late Maastrichtian	Nannofossil chalk, foraminiferal-nannofossil chalk, limestone, and conglomerate	74	Manivit and Feinberg (1984)	9
530A	1980	19°11.26′S 09°23.15′E	Southwest Angola Basin	4629	Early Campanian to Late Maastrichtian	Mudstone, limestone, sandstone, claystone, and siltstone	115	Keating and Herrero-Bervera (1985)	10
661A	1986	09°26.81′S 19°23.116′E	Kane Gap	4005.8	Late Campanian to Late Maastrichtian	Zeolite, clayey nannofossil ooze, nannofossil clay, and zeolitic clay	32	No data	6
690C	1987	65°9.621′S 01°12.285′E	Falkland Plateau	2914	Late Campanian to Late Maastrichtian	Foraminifer-bearing muddy nannofossil chalk, muddy nannofossil chalk, calcareous claystone, clayed chalk, and muddy chalk	41	Hamilton (1990)	12
700B	1987	51°31.977′S 30°16.688′W	Georgia Basin	3601	Early/Late Campanian? to Late Maastrichtian	Micritic limestone, clay-bearing micritic limestone, and limestone	67	Hailwood and Clement (1991)	13
1258A	2003	09°26.00′N 54°43.00′W	Demerara Rise	3192.2	Late Campanian to Late Maastrichtian	Clayey nannofossil chalk, nannofossil chalk, foraminiferal-nannofossil chalk, clayey calcareous chalk, and limestone	77	Erbacher et al. (2004)	7

close to each other between provinces that the events are not significantly diachronous.

Our zones were numbered from the top of the Mesozoic downward. This is to allow additional numbered zones to be added afterwards for older, as-yet unnumbered stratigraphic intervals.

3. Results of biostratigraphic zonations

The biostratigraphical ranges presented here, when compared to magnetostratigraphic data published in the original site reports, demonstrate that some of the bio-horizons of Watkins et al. (1996) and Burnett et al. (1998) should be used carefully for South Atlantic Ocean biostratigraphy (see Sections 4.2.1 and 4.2.2, Figs. 3 and 4). Taking into account the high degree of diachronism observed in this wide area, we suggest three new latitudinal zonations (low-, mid- and high-latitudes) tied to the standard magnetostratigraphic timescale (Fig. 3).

The need for proposing new biozonations for the Campanian–Maastrichtian interval of the South Atlantic Ocean comes from our finding that many of the zonal markers were in a different order compared with the zonations of Burnett et al. (1998), and Watkins et al. (1996), or were significantly diachronous between provinces. Furthermore, it is not possible to correlate our calcareous nannofossil bio-horizons to those zonations, as they are not tied to the paleomagnetic time scale. Therefore, it would be misleading to use previously defined zonal names from other regions. Although our low- and mid-latitude zonations utilize many of the same species as the Burnett et al. (1998) zonation, there are a number of species that are specific to each province, the bio-horizons are mostly diachronous, and sometimes occur in a different order. The zonations of Watkins et al. (1996) and Burnett et al. (1998), discussed during the description of the zones, are shown in Fig. 4.

Some information about each site including the stratigraphic ranges of selected species (black color for markers used herein and gray color for markers applied in other zonations), geomagnetic polarity chron records, core recovery, position of the studied samples and previous nannofossil studies, can be seen as Online Supplementary data (Figs. S1 to S9).

3.1. South Atlantic Ocean Low-latitude region (SAL)

The proposed zones for the South Atlantic Ocean Low-latitude region are based on three sites: 354, 661A, and 1258A (Figs. S1–S3). The prefix "SAL" stands for "South Atlantic Low-latitude region". Most of the markers used to define this zonation are the same as described by Burnett et al. (1998). However, we cannot correlate their zonation with ours since most of our bio-horizons have a high-degree of diachroneity and their zonation lacks accurate magnetostratigraphic control.

3.1.1. SAL1 nannofossil zone
Definition: Top defined by the LO of unreworked, non-survivor Cretaceous taxa and base defined by the FO of *Micula prinsii*.

Age: Late Maastrichtian (top/middle part of Chron C29r to top of Chron C30r).

Remarks: The FO of *M. prinsii* has been placed inside Chron C29r by some authors (Manivit and Feinberg, 1984; Thibault and Gardin, 2006, 2007; Gardin et al., 2012; Thibault et al., 2012). We place this bio-horizon at the top of Chron C30r in Hole 1258A. Following a similar pattern as described by Thibault et al. (2010) for *M. murus*, this species seems to migrate from the Equatorial Atlantic to the South Atlantic Ocean (see Section 4.2.2).

Stratigraphic distribution: From 103.33 to 109.80 mbsf at Hole 661A (Fig. S2), and from 255.63 to 267.85 mbsf at Hole 1258A (Fig. S3).

3.1.2. SAL2 nannofossil zone
Definition: Top defined by the FO of *M. prinsii* and base defined by the FO of *Ceratolithoides kamptneri*.

Age: Late Maastrichtian (top of Chron C30r to middle part/base of Chron C31n).

Remarks: At Hole 1258A *C. kamptneri* occurs below the magnetostratigraphic chronozone (Chron C30n) described by several authors (Thibault and Gardin, 2007; Thibault et al., 2012), following the same pattern of *M. prinsii* in this site having an earlier occurrence in comparison to mid-latitude sites.

Stratigraphic distribution: From 109.80 to 111.35 mbsf at Hole 661A (Fig. S2), and from 267.85 to 289.10 mbsf at Hole 1258A (Fig. S3).
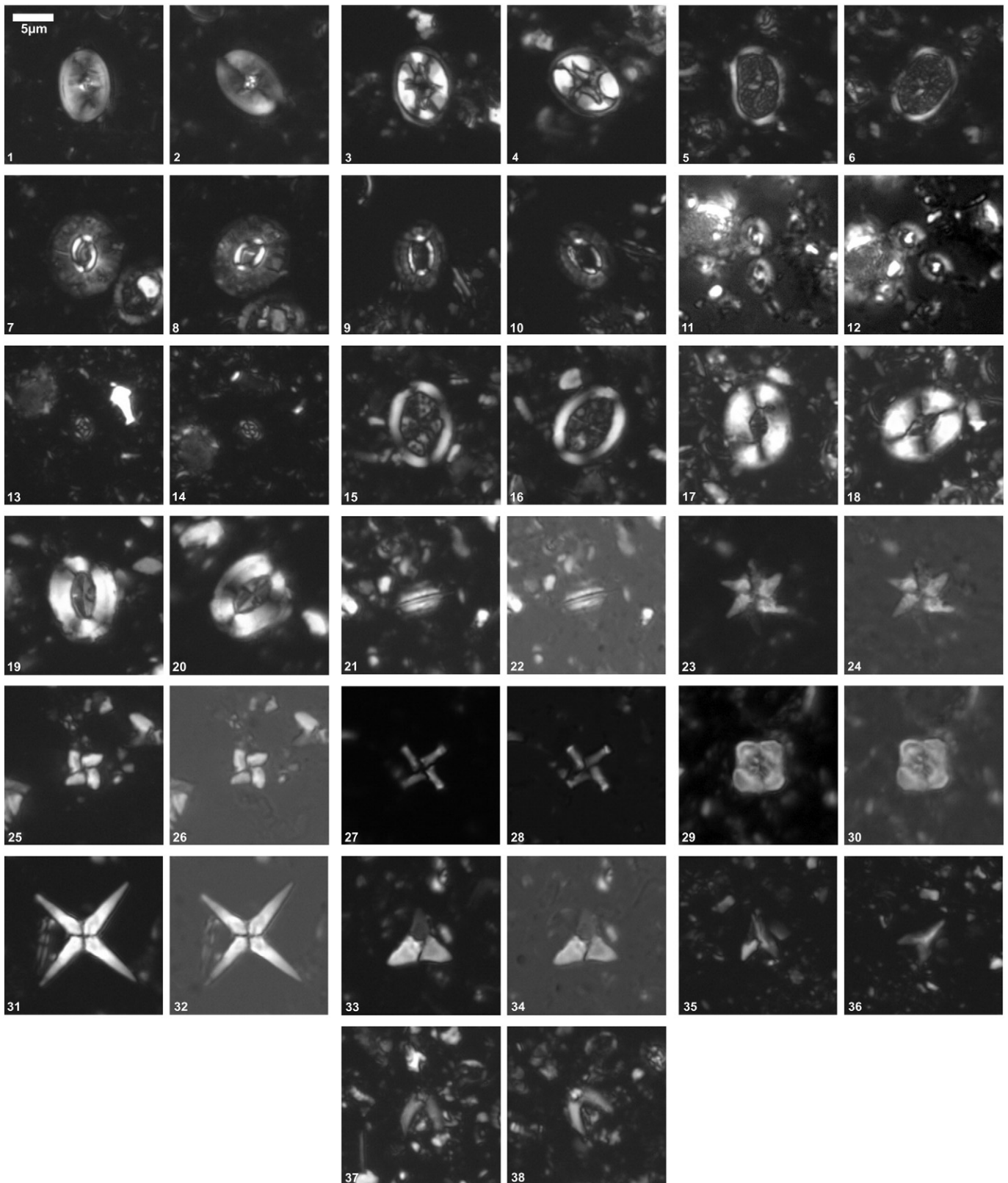
Fig. 2. 1/2, *Reinhardtites levis* (Hole 690C/21-1); 3/4, *Eiffellithus eximius* (Hole 530A/78-7); 5/6, *Nephrolithus corystus* (Hole 690C/20-2); 7/8, *Biscutum coronum* (Hole 690C/21-2); 9/10, *Biscutum magnum* (Site 511/24-7); 11/12, *Gephyrobiscutm diabolum* (Site 511/31-1); 13/14, (Site 511/33-6); 15/16, *Arkhangelskiella cymbiformis* (Hole 690C/19-3); 17/18, *Broinsonia parca constricta* (Hole 690C/19-4); 19/20, *Broinsonia parca parca* (Hole 530A/77-2); 21/22, *Lithraphidites quadratus* (Hole 1258A/31-4); 23/24, *Lithastrinus grillii* (Hole 530A/79-5); 25/26, *Micula murus* (Hole 530A/51-4); 27/28, *Micula prinsii* (Hole 661A/13-1); 29/30, *Quadrum svabenickae* (Site 356/34-2); 31/32, *Uniplanarius sissinghii* (Hole 661A/18-2); 33/34, *Uniplanarius trifidus* (Hole 661A/17-1); 35/36, *Ceratolithoides aculeus* (Hole 1258A/35-2); 37/38, *Ceratolithoides kamptneri* (Hole 1258A/31-4).
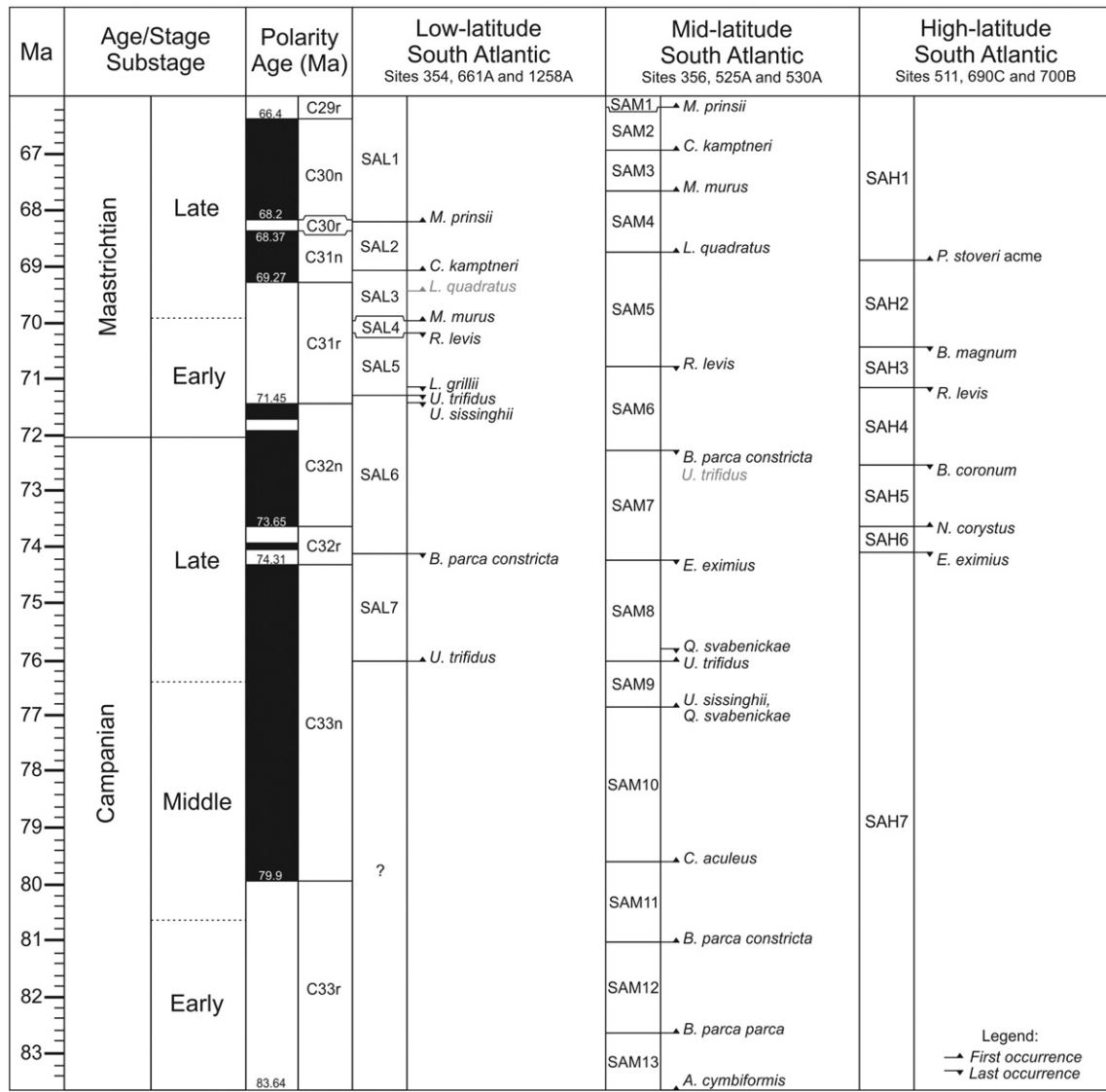
Fig. 3. Summary of the new Campanian–Maastrichtian calcareous nannofossil biozonation for the South Atlantic Ocean, shown compared with the paleomagnetic time scale of Gradstein et al. (2012).

3.1.3. SAL3 nannofossil zone

Definition: Top defined by the FO of *C. kamptneri* and base defined by the FO of *M. murus*.

Age: Late Maastrichtian (middle part/base of Chron C31n to middle part/top of Chron C31r).

Remarks: The FO of *Lithraphidites quadratus* was identified within this zone at Hole 1258A, nevertheless this biological event was not included in our zonation because of the reversed order between this occurrence and the FO of *M. murus* (compared with the global distribution of these two species). The same reverse order of bio-horizons was described by Self-Trail (2001) in the western Atlantic region, Lees and Bown (2005) in the northwest Pacific Ocean, and Thibault and Gardin (2006) for the same hole studied herein (1258A). We did not recover *L. quadratus* at Hole 661A, despite the Manivit (1984) comment about the rare presence of poorly preserved fragments of this species. The FO of *M. murus* (base of this zone) usually lies within Chron C30n (Manivit and Feinberg, 1984; Thibault and Gardin, 2007; Gardin et al., 2012; Thibault et al., 2012). Nevertheless, we identified this bio-horizon in the middle part/top of Chron C31r at Hole 1258A.

Stratigraphic distribution: From 111.35 to 116.35 mbsf at Hole 661A (Fig. S2), and from 289.10 to 303.82 mbsf at Hole 1258A (Fig. S3).

3.1.4. SAL4 nannofossil zone

Definition: Top defined by the FO of *M. murus* and base defined by the LO of *Reinhardtites levis*.

Age: Early/Late Maastrichtian (top to middle part of Chron C31r).

Remarks: It appears as though the LO of *R. levis* within the middle of Chron C31r at Hole 1258A correlates well with the position of this bio-horizon in other locations (Gardin et al., 2012; Pérez-Rodríguez et al., 2012). The remarkable lower position of the LO of *M. murus* at Hole 1258A prevents the recognition of a consistent FO of *L. quadratus* in the low latitude South Atlantic Ocean.

Stratigraphic distribution: From 116.35 to 128.84 mbsf at Hole 661A (Fig. S2), and from 303.82 to 306.80 mbsf at Hole 1258A (Fig. S3).

3.1.5. SAL5 nannofossil zone

Definition: Top defined by the LO of *R. levis* and base defined by the LO of *Uniplanarius trifidus*.

Age: Early Maastrichtian (middle to base of Chron C31r).

Remarks: The LO of *U. trifidus* occurs close to the boundary between chrons C31r and C32n at Hole 1258A, in the same pattern as reported from other localities around the world (e.g., Manivit and Feinberg, 1984; Gardin et al., 2012). The LO of *Lithastrinus grillii* occurs within
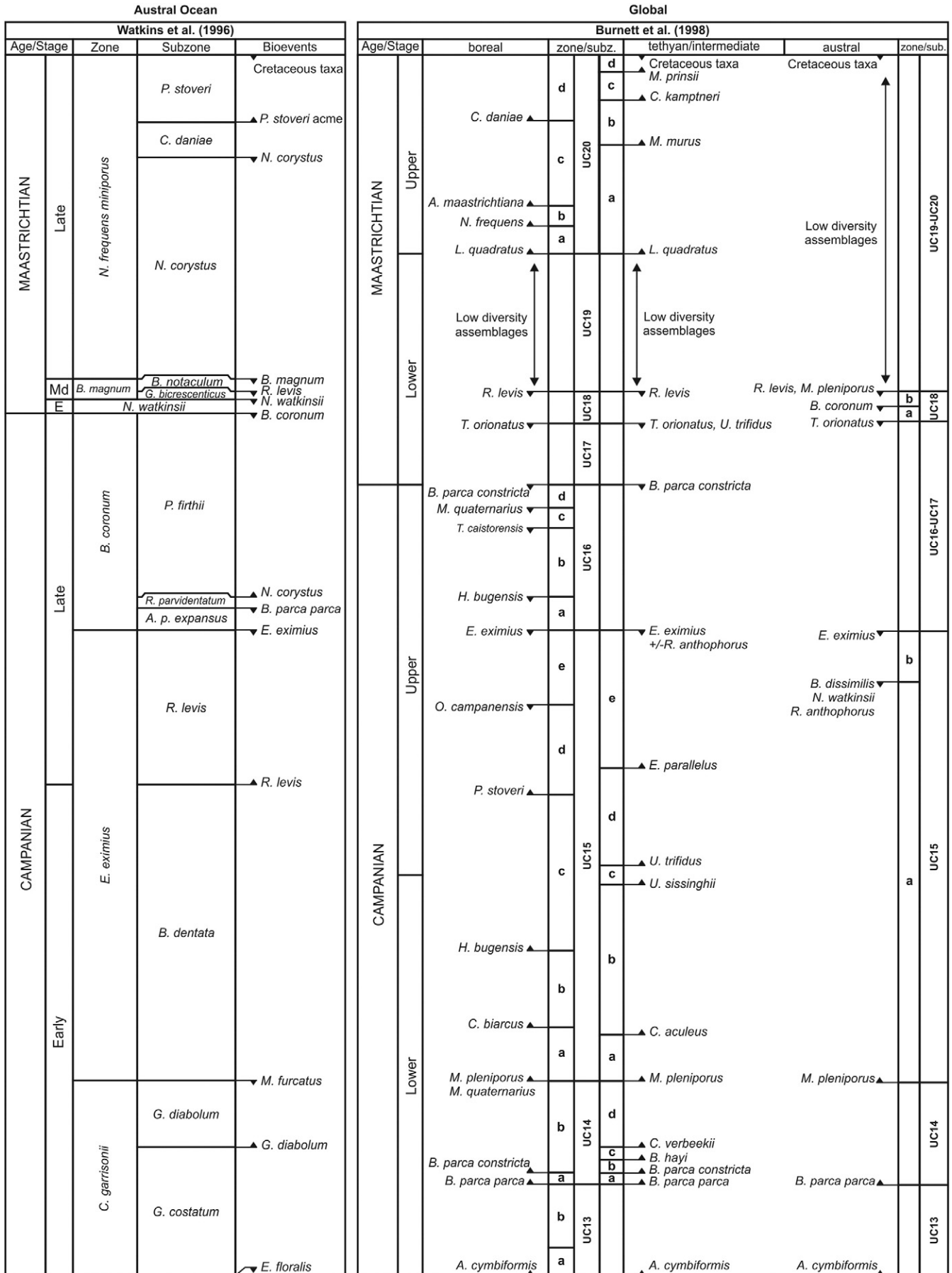
Fig. 4. Campanian and Maastrichtian zonations of Watkins et al. (1996) and Burnett et al. (1998).

this zone in both holes (1258A and 661A) close to the LO of *U. trifidus* at the base of Chron C31r.

Stratigraphic distribution: From 128.84 to 131.84 mbsf at Hole 661A (Fig. S2), and from 306.80 to 327.34 mbsf at Hole 1258A (Fig. S3).

3.1.6. SAL6 nannofossil zone

Definition: Top defined by the LO of *U. trifidus* and base defined by the LO of *Broinsonia parca constricta*.

Age: Early Maastrichtian to late Campanian (base of Chron C31r to the middle part of Chron C32n).

Remarks: According to Burnett et al. (1998) the LO of *B. parca constricta* defines the Campanian/Maastrichtian boundary. Some authors suggest that this bio-horizon was younger, during the early– middle part of the late Maastrichtian, within Chron C31r (Gardin et al., 2012; Pérez-Rodríguez et al., 2012; Thibault et al., 2012). We identified the LO of *B. parca constricta* at Hole 1258A as older than these previous studies, in the middle of Chron C32r, which is probably due to migration patterns (see Section 4.2). The LO of *Uniplanarius sissinghii* occurs within this zone in both holes (1258A and 661A), close to the LO of *U. trifidus* and at the limit between chrons C31r and C32n.

Stratigraphic distribution: From 131.84 to 155.85 mbsf at Hole 661A (Fig. S2), and from 327.34 to 364.64 mbsf at Hole 1258A (Fig. S3).

3.1.7. SAL7 nannofossil zone

Definition: Top defined by the LO of *B. parca constricta* and base defined by the FO of *U. trifidus.*

Age: Late Campanian (middle part of Chron C32r to upper-middle part of Chron C33n).

Remarks: The FO of *U. trifidus* occurs within Chron C33n at Hole 1258A. Although the FO of this species is not detected at Hole 661A, it co-occurs with *B. parca constricta* in the lowest sample at 155.85 mbsf. The LO of *B. parca constricta* is present at both Holes 1258A and 661A, within Chron C32r at Hole 1258A. Unlike Burnett et al. (1998), we did not find the LOs of *Eiffellithus eximius* and *Reinhardites anthophorus* and the FO of *Eiffellithus parallelus* in this zone. At Hole 1258A these three species occur in the wrong position in comparison to Burnett et al. (1998), and not all of them occur at Hole 661A (apart for one sample containing *R. anthophorus*). Unfortunately, there are no samples representative of the early to mid-Campanian for low latitudes, therefore this interval was marked by a questionable point on our summary of the biostratigraphic zonation (Fig. 3).

Stratigraphic distribution: From 364.64 to 382.20 mbsf at Hole 1258A (Fig. S3).

3.2. South Atlantic Ocean Mid-latitude region (SAM)

Our proposed zones for the mid-latitude South Atlantic Ocean region are suggested based on three sites: 356, 525A, and 530A (Figs. S4–S6). The prefix "SAM" stands for "South Atlantic Mid-latitude region". As for the SAL zonation, most of the markers used are the same as described in Burnett et al. (1998). However, most of the events appear to have a high-degree of diachroneity between ocean basins and latitudinal zones, therefore, as mentioned previously, we do not use their zonal names.

3.2.1. SAM1 nannofossil zone

Definition: Top defined by the LO of unreworked, non-survivor Cretaceous taxa and base defined by the FO of *M. prinsii*.

Age: Late Maastrichtian (top to base of Chron C29r).

Remarks: In the mid-latitude South Atlantic Ocean, the FO of *M. prinsii* is within Chron C29r, which appears to correlate well with results from other ocean basins (south-eastern Atlantic Ocean, Manivit and Feinberg, 1984 and Thibault and Gardin, 2007; equatorial Atlantic Ocean, Thibault and Gardin, 2006; Umbria-Marche Basin, Italy, Gardin et al., 2012; and eastern Indian Ocean, Thibault et al., 2012). However

this datum is diachronous between the mid- and low-latitude South Atlantic Ocean.

Stratigraphic distribution: From 410.70 to 418.77 mbsf at Site 356 (Fig. S4), from 452.30 to 457.63 mbsf at Hole 525A (Fig. S5), and from 592.80 to 594.25 mbsf at Hole 530A (Fig. S6).

3.2.2. SAM2 nannofossil zone

Definition: Top defined by the FO of *M. prinsii* and base defined by the FO of *C. kamptneri*.

Age: Late Maastrichtian (base of Chron C29r to top/middle part of Chron C30n).

Remarks: The FO of *C. kamptneri* was identified within the middle part/top of Chron C30n at Hole 525A. The magnetostratigraphic record for Hole 530A (Keating and Herrero-Bervera, 1985) unfortunately is not sufficiently well-resolved to subdivide chrons C30n and C31n. Herein, the FO of *C. kamptneri* is placed within the top part of the undifferentiated Chron C30n–C31n. Taking into account the magnetostratigraphic compilation (Gradstein et al., 2012) that shows a wider Chron C30n and a smaller C31n, we suggest this bio-horizon occurred close to the middle part/top of Chron C30n.

Stratigraphic distribution: From 418.77 to 424.77 mbsf at Site 356 (Fig. S4), from 457.63 to 462.32 mbsf at Hole 525A (Fig. S5), and from 594.25 to 600.75 mbsf at Hole 530A (Fig. S6).

3.2.3. SAM3 nannofossil zone

Definition: Top defined by the FO of *C. kamptneri* and base defined by the FO of *M. murus*.

Age: Late Maastrichtian (top/middle part to middle part/base of Chron C30n).

Remarks: The FO of *M. murus* was identified in the middle-base of Chron C30n at Hole 525A. At Hole 530A, this species first occurs in the middle part/top of the undifferentiated Chron C30n–C31n. Using the same criteria described in the previous zone (see SAM2) we suggest that this bio-horizon occurs also in the middle part/base of Chron C30n.

Stratigraphic distribution: From 424.77 to 445.16 mbsf at Site 356 (Fig. S4), from 462.32 to 468.71 mbsf at Hole 525A (Fig. S5), and from 600.75 to 605.22 mbsf at Hole 530A (Fig. S6).

3.2.4. SAM4 nannofossil zone

Definition: Top defined by the FO of *M. murus* and base defined by the FO of *L. quadratus*.

Age: Late Maastrichtian (middle part/base of Chron C30n to middle part of Chron C31n).

Remarks: The FO of *L. quadratus* is within the middle part of Chron C31n at Hole 5250A, a pattern that matches some studies from other ocean basins (Umbria–Marche Basin, Italy, Gardin et al., 2012; northern Spain, Pérez-Rodríguez et al., 2012).

Stratigraphic distribution: From 445.16 to 457.31 mbsf at Site 356 (Fig. S4), and from 468.71 to 480.80 mbsf at Hole 525A (Fig. S5).

3.2.5. SAM5 nannofossil zone

Definition: Top defined by the FO of *L. quadratus* and base defined by the LO of *R. levis*.

Age: Late to early Maastrichtian (middle part of Chron C31n to middle part/base of Chron C31r).

Remarks: The LO of *R. levis* was only recovered at Hole 525A, within the middle part/base of Chron C31r. At Sites 356 and 530A it seems that this bio-horizon was lost due to coring gaps (see Figs. S4 and S6).

Stratigraphic distribution: From 480.80 to 509.30 mbsf at Hole 525A (Fig. S5).

3.2.6. SAM6 nannofossil zone

Definition: Top defined by the LO of *R. levis* and base defined by the LO of *B. parca constricta*.

Age: Early Maastrichtian (middle part/base of Chron C31r to top/ middle part of Chron C32n).

Remarks: Unfortunately we could not identify a consistent LO of *U. trifidus* for the mid latitudes in the South Atlantic Ocean. At all sites analyzed here, this bio-horizon occurs together with the LO of *B. parca constricta*. At Site 356 the LO of *U. trifidus* occurs at the same level as LOs of *B. parca constricta*, *E. eximius*, *R. levis*, and *U. sissinghii*, just below a large coring gap of ~20 m. At Hole 525A the LO of *U. trifidus* occurs in the same sample of the LO of *B. parca constricta* in a continuous section. At Hole 530A the LO of *U. trifidus* occurs together with the LOs of *B. parca constricta*, *R. levis*, and *U. sissinghii* also below a recovery gap of ~7 m. This pattern indicates the occurrence of a possible unconformity at mid latitudes during the early Maastrichtian. The LO of *B. parca constricta* at Holes 525A and 530A lies within the middle part/ top of Chron C32n.

Stratigraphic distribution: From 509.30 to 522.89 mbsf at Hole 525A (Fig. S5).

3.2.7. SAM7 nannofossil zone

Definition: Top defined by the LO of *B. parca constricta* and base defined by the LO of *E. eximius*.

Age: Late Campanian (top/middle part of Chron C32n to base of Chron C32r).

Remarks: The LOs of *E. eximius* and *R. anthophorus* occur together within the base of Chron C32r at Hole 530A. Unfortunately, this bio-horizon was not recovered at Hole 525A and cannot be distinguished at Site 356 due to a large coring gap of ~20 m.

Stratigraphic distribution: From 522.89 to the base of the studied section at Hole 525A (Fig. S5) 638.56 to 676.77 mbsf at Hole 530A (Fig. S6).

3.2.8. SAM8 nannofossil zone

Definition: Top defined by the LO of *E. eximius* base defined by the FO of *U. trifidus*.

Age: Late Campanian (base of Chron C32r to top/middle part of Chron C33n).

Remarks: The LO of *Quadrum svabenickae* lies within this zone close to the FO of *U. trifidus*, and could be identified at both sites (356 and 530A). The FO of *U. trifidus* is the only bio-horizon that seems to correlate well with the SAL (low-latitude) zonation described above. We did not find *E. parallelus* at Hole 530A, but at sites 356 and 525A the FO of this species is younger than described in Burnett et al. (1998).

Stratigraphic distribution: From 485.27 to 492.74 mbsf at Site 356 (Fig. S4), and from 676.77 to 708.25 mbsf at Hole 530A (Fig. S6).

3.2.9. SAM9 nannofossil zone

Definition: Top defined by the FO of *U. trifidus* and base defined by the FO of *U. sissinghii*.

Age: Late to middle Campanian (top to middle part of Chron C33n).

Remarks: The FOs of *U. sissinghii* and *Q. svabenickae* were identified at the same level at Hole 530A, suggesting that both can mark the base of this zone. Site 356 seems to show the same pattern, since we recovered both species together in the last sample analyzed (521.27 mbsf). According to the original Site 356 report by Perch-Nielsen (1977), there is a sedimentary gap below this sample, followed by Santonian strata.

Stratigraphic distribution: From 492.74 to 521.27 mbsf at Site 356 (Fig. S4), and from 708.25 to 725.75 mbsf at Hole 530A (Fig. S6).

3.2.10. SAM10 nannofossil zone

Definition: Top defined by the FO of *U. sissinghii* base defined by the FO *Ceratolithoides aculeus*.

Age: Middle Campanian (middle part to base of Chron C33n).

Remarks: The FO of *C. aculeus*, within the base of Chron C33n, was identified only at Hole 530A (single mid-latitude hole studied herein with early–mid Campanian recovery), and seems to correlate well with the position of this bio-horizon in Burnett et al. (1998).

Stratigraphic distribution: From 725.75 to 781.25 mbsf at Hole 530A (Fig. S6).

3.2.11. SAM11 nannofossil zone

Definition: Top defined by the FO of *C. aculeus* and base defined by the FO of *B. parca constricta*.

Age: Early to middle Campanian (base of Chron C33n to top/middle part of Chron C33r).

Remarks: We could not identify *Misceomarginatus pleniporus* or *Ceratolithoides verbeekii* at either site, which are species used as early Campanian markers in the zonation of Burnett et al. (1998). *Bukryaster hayi* was recovered only at Hole 530A and its FO is younger than described in Burnett et al. (1998).

Stratigraphic distribution: From 781.25 to 844.25 mbsf at Hole 530A (Fig. S6).

3.2.12. SAM12 nannofossil zone

Definition: Top defined by the FO of *B. parca constricta* and base defined by the FO of *Broinsonia parca parca*.

Age: Early Campanian (within Chron C33r).

Remarks: The FO of *B. parca parca* occurs in the middle part/base of Chron C33r at Hole 530A. The same bio-horizons, used here to define Zone SAM12, were also used by Burnett et al. (1998) to define the early Campanian.

Stratigraphic distribution: From 844.25 to 866.75 mbsf at Hole 530A (Fig. S6).

3.2.13. SAM13 nannofossil zone

Definition: Top defined by the FO of *B. parca parca* base defined by the FO of *Arkhangelskiella cymbiformis*.

Age: Early Campanian (middle part/base to base of Chron C33r).

Remarks: The FO of *A. cymbiformis* lies within the base of Chron C33r. This bio-horizon defines the limit of the Campanian/Santonian boundary in Burnett et al. (1998).

Stratigraphical distribution: From 866.75 to 879.25 mbsf at Hole 530A (Fig. S6).

3.3. South Atlantic Ocean High-latitude region (SAH)

The biozonation for the South Atlantic Ocean at the high-latitude region is based on three sites: 511, 690C, and 700B (Figs. S7–S9). The prefix "SAH" stands for "South Atlantic High-latitude region". Some markers are the same as described in the Southern Ocean zonation of Watkins et al. (1996). We use different zonal names because many of the markers were not recovered, showed diachronous range, or bio-horizons occur in a different order compared to Watkins et al. (1996) and Burnett et al. (1998).

3.3.1. SAH1 nannofossil zone

Definition: Top defined by the LO of unreworked, non-survivor Cretaceous taxa and base defined by the FO of the *Prediscosphaera stoveri* acme.

Age: Late Maastrichtian (top of Chron C29r to middle part of Chron C31n).

Remarks: The acme of *P. stoveri* in Chron C31n occurs at Holes 690C and 700B, and corresponds to an interval where the abundance of this marker species increases suddenly (see Supplementary data Tables S7 and S8).

Stratigraphic distribution: From 247.60 to 264.07 mbsf at Hole 690C (Fig. S8), and from 331.40 to 332.94 mbsf at Hole 700B (Fig. S9).

3.3.2. SAH2 nannofossil zone

Definition: Top defined by the FO of the *P. stoveri* acme and base defined by the LO of *Biscutum magnum*.

Age: Late to early Maastrichtian (middle part of Chron C31n to middle part of Chron C31r).

Remarks: Within this zone Watkins et al. (1996) described the *Nephrolithus corystus* Subzone, based on the LO of *N. corystus*. We identified a diachronous LO for this species between Holes 690C (base of

Chron C31n) and 700B (with its range continuing to the end of the section within Chron C30n). The LO of *B. magnum* seems to be consistent at both sites in the middle part of Chron C31r.

Stratigraphic distribution: From 264.07 to 277.80 mbsf at Hole 690C (Fig. S8), and from 332.94 to 347.23 mbsf at Hole 700B (Fig. S9).

3.3.3. SAH3 nannofossil zone

Definition: Top defined by the LO of *B. magnum* and base defined by the LO of *R. levis*.

Age: Early Maastrichtian (middle part to base of Chron C31r).

Remarks: The LO of *R. levis* lies at the base of Chron C31r at Holes 690C and 700B.

Stratigraphic distribution: From 277.80 to 281.82 mbsf at Hole 690C (Fig. S8), and from 347.23 to 355.20 mbsf at Hole 700B (Fig. S9).

3.3.4. SAH4 nannofossil zone

Definition: Top defined by the LO of *R. levis* and base defined by the LO of *Biscutum coronum*.

Age: Early Maastrichtian to late Campanian (base of Chron C31r to top/middle part of Chron C32n).

Remarks: Watkins et al. (1996) identified the *Neocrepidolithus watkinsii* subzone within this zone, based on the LO of *N. watkinsii*. In our study, the LO of this species at Holes 690C and 700B is diachronous and inconsistent. The LO of *B. coronum* lies within the middle part/top of Chron C32n at Holes 690C and 700B.

Stratigraphic distribution: From 281.82 to 293.05 mbsf at Hole 690C (Fig. S8), and from 355.20 to 367.75 mbsf at Hole 700B (Fig. S9).

3.3.5. SAH5 nannofossil zone

Definition: Top defined by the LO of *B. coronum* and base defined by the FO *N. corystus*.

Age: Late Campanian (top/middle part of Chron C32n to chrons C32n/C32r).

Remarks: The FO of *N. corystus* occurs in different chrons at Holes 690C and 700B (base of Chron C32r in the former and middle part/top of Chron C32n in the latter). However, the age of this event is probably the same, as is the order of the other bio-horizons at Site 511. This pattern allowed us to place the FO of this species between chrons C32r and C32n.

Stratigraphic distribution: From 195.99 to 209.10 mbsf at Site 511 (Fig. S7), from 293.05 to 307.15 mbsf at Hole 690C (Fig. S8), and from 367.75 to 369.24 mbsf at Hole 700B (Fig. S9).

3.3.6. SAH6 nannofossil zone

Definition: Top defined by the FO *N. corystus* and base defined by the LO of *E. eximius*.

Age: Late Campanian (chrons C32n/C32r to top/middle part of Chron C32r).

Remarks: The LO of *E. eximius* was delineated at Sites 511 and 700B, the latter of which shows that this bio-horizon lies in the middle part/top of Chron C32r. Watkins et al. (1996) described the *Aspidolithus parcus expansus* subzone within this zone, based on the LO of *A. parcus* (= *B. parca*) and related forms. In our study, the occurrences of these species at high-latitudes sites are scarce and diachronous.

Stratigraphic distribution: From 209.10 to 230.21 mbsf at Site 511 (Fig. S7), and from 369.24 to 416.70 mbsf at Hole 700B (Fig. S9).

3.3.7. SAH7 nannofossil zone

Definition: Interval below the LO *E. eximius*.

Age: Early to late Campanian (middle part of Chron C32r to base of Chron C33n).

Remarks: Site 511 recovered a well-constrained Early to Late Campanian section, just below the LO of *E. eximius*. Unfortunately, there is no magnetostratigraphic record for this site, and we have no other section over this time period so we cannot locate these bio-horizons in our high-latitude zonation. Two main bio-horizons identified at Site 511,

the FOs of *Gephyrobiscutum diabolum* and *R. levis*, were tied to the early to late Campanian by Watkins et al. (1996). Taking into account the position of the LO of *E. eximius*, our new zonation would probably indicate the same ages as the one of Watkins et al. (1996) for these two bio-horizons.

Stratigraphical distribution: From 230.21 to 349.20 mbsf at Site 511 (Fig. S7), and from 416.70 to 445.26 mbsf at Hole 700B (Fig. S9).

4. Discussion

In the magnetostratigraphic interpretation for Hole 1258A, Erbacher et al. (2004) were not confident with the magnetostratigraphic signal of the lower part of our section and suggested that age assignments would probably change with new biostratigraphic data. We suggest that Core 41 and the middle part/base of Core 40 belong to Chron C33n, and not to Chron C34n as suggested in the original study. This is mainly due to the fact that there are no species indicative of a Santonian age for this interval. The magnetostratigraphic reversal between the middle/top part of Core 40 to the base of Core 38 is assigned to Chron C32r, and from the middle/top part of Core 38 to the base of Core 35 to Chron C32n. In this way the short Chron C33r?, interpreted by Erbacher et al. (2004), is suggested here to be part of the Chron C32n, improving correlation to Gradstein et al. (2012), who shows Chron C33n as a long-lasting interval.

A similar situation is seen in Hole 700B where Hailwood and Clement (1991) interpretations are inconsistent with the biostratigraphic data described herein. Those authors attributed the last two cores of our section (49 and 50) to Chron C34n, Santonian in age, while nannofossil distribution observed herein suggests these two cores should be assigned to Chron C33n. The interval between Cores 46 to 40, identified as Chron C33n to Chron C32n by Hailwood and Clement (1991), are herein suggested to span only Chron C32n. In this case the reversal defined as Chron C32r by those authors is just the short reversal within Chron C32n. This interpretation matches better with the standard magnetostratigraphy of Gradstein et al. (2012).

4.1. Comparisons with previous biozonation schemes

One of the primary findings of this study is that many of the zonal markers for the Campanian and Maastrichtian identified by Watkins et al. (1996) at high latitudes and Burnett et al. (1998) in the Indian Ocean are not consistently applicable to the South Atlantic Ocean. We do not think that water depth or proximity to land (which commonly limits the occurrence of species due to changes in salinity and nutrients (Ziveri et al., 2004; Winter et al., 1994)) significantly affected species ranges, as all our sites are located in deep water today (Table 1) and were probably not located at shelf depths during the Late Cretaceous.

Specifically for low and mid latitudes, we could not identify the species *C. verbeekii* and *M. pleniporus*, both early Campanian markers of Burnett et al. (1998). The species *B. hayi* and *E. parallelus*, early and late Campanian markers occur at our low- and mid-latitude sites (Holes 661A and 530A), although their occurrences are scarce and diachronous (see Figs. S2 and S6A–C) when compared to the zonation of Burnett et al. (1998). At low latitudes, we could not utilize the biostratigraphic markers *L. quadratus* and *E. eximius*. *L. quadratus* first occurs at Site 354 where the recovery of nannofossils was poor, giving us no information about the order of the bio-horizons. *L. quadratus* was also recovered at Hole 1258A, where we identified this species in a reversed stratigraphic order with *M. murus*. The LO of *E. eximius* was identified only at Hole 1258A and appears to be in a different position in relation to Burnett et al. (1998). In addition to the absence of some markers, the correlation of our bio-horizons with magnetostratigraphic data shows high diachronism between low and mid latitudes, particularly for late Maastrichtian species, as recently demonstrated for *M. murus* by Thibault et al. (2010).

For high latitudes, Burnett et al. (1998) high-latitude zonation is not applicable for the South Atlantic Ocean, where only four of their eleven bio-horizons occur (FO of Cenozoic taxa and LOs of *R. levis*, *B. coronum*, and *E. eximius*). On the other hand, Watkins et al. (1996) provided a Southern Ocean zonation based on some of the sites studied herein in addition to sites drilled in the Indian Ocean. Based on our analyses, some bio-horizons described by Watkins et al. (1996) seem to be diachronous (see Figs. S8 and S9) or do not occur in the South Atlantic Ocean (LOs of *N. corystus*, *N. watkinsii*, and *B. parca*), thus we did not use those markers in our new zonation.

Site 511 recovered levels below the LO of *E. eximius* (from 230.21 to 350.70 mbsf). In these samples, it was possible to identify two of Watkins et al. (1996) bio-horizons probably dated as mid–early Campanian (the FOs of *R. levis* and *G. diabolum*). Taking into account our methodology to describe the new zones, based on more than one site or tied to magnetostratigraphy, we do not define zones with these two bio-horizons although further work may prove them suitable.

4.2. Late Cretaceous climate change and nannofossil migrations

The vertical and horizontal distribution of living coccolithophores in the oceans is controlled by several factors, including salinity, temperature, nutrients and productivity, which vary with latitude (temperature and light intensity) and ocean currents (Ziveri et al., 2004; Winter et al., 1994). Dominant coccolithophores in the modern Atlantic Ocean show strong regional distributions that appear to be largely controlled by temperature and availability of nutrients (Ziveri et al., 2004). Many of the species show different distributions between the North and South Atlantic Oceans, although others show similarities. Understanding the preferences of modern species, however, has become more difficult with the recent identification of subspecies within many previously accepted broad morphological groups (Ziveri et al., 2004). For extinct nannofossils there are even more uncertainties in assigning ecological preferences of taxa and a careful taxonomic work, coupled with paleobiogeographic studies, is needed. Several studies of Upper Cretaceous sections interpret the occurrences of certain taxa as controlled by latitude and, consequently, related to climate (Wind, 1979; Thierstein, 1981; Roth and Krumbach, 1986; Wise, 1988; Watkins, 1989; Shafik, 1990; Erba, 1992; Lees, 2002; Erba, 2004; Lees et al., 2005; Mutterlose et al., 2005; Watkins and Self-Trail, 2005; Hardas et al., 2012; Thibault and Gardin, 2006; Thibault et al., 2010; Linnert et al., 2014; Linnert and Mutterlose, 2015; Thibault and Husson, 2016). Recent works have made particular progress, and some species preferences for distinct paleoecological conditions have been demonstrated as useful for constraining climatic and oceanographic changes (Lees, 2002; Thibault et al., 2010; Linnert et al., 2014).

4.2.1. Campanian

Our findings show that high-latitude (Southern Ocean and Antarctic) zonal markers are quite different from those of the mid and low latitudes in the South Atlantic Ocean, confirming the different floral provinces suggested by many authors. There is just one bio-horizon synchronous across these latitudes, the LO of *E. eximius* in the late Campanian (Fig. 3). This indicates that a strong latitudinal gradient, probably related to temperature, occurred during the Campanian. Global deep-ocean foraminiferal $\delta^{18}O$ records (Friedrich et al., 2012), controlled by changes in temperature and salinity, indicates that a continuous global cooling trend during the Coniacian and Santonian persisted throughout the early and mid Campanian. Sea-surface temperatures at the high-latitude Site 511 (Huber et al., 1995, 2002) diverged from temperatures at low-latitude locations such as the Gulf of Mexico (Linnert et al., 2014) during this time interval, confirming the increased latitudinal gradient. At about 77 Ma, deep waters appear to have started warming (Friedrich et al., 2012), which could account for the similarity of the bio-horizon *E. eximius* at this time (Fig. 3). Comparison of mid- to low-latitude differences during the early–mid Campanian is not possible

due to the poor recovery of low-latitude assemblages in our study. However, the FO of *U. trifidus* indicates that there may have been some similarity between both latitudes in the late Campanian supporting the idea that this warming, and the possible diminution of the latitudinal gradients, may have contributed to the observed pattern in nannofossil distributions. Interestingly, *B. parca constricta* disappears much earlier at low latitudes during the late Campanian (~74 Ma as opposed to ~72 Ma in the mid-latitude region). Although there is no latitudinal control defined for this species yet (Lees, 2002), we suggest that *B. parca constricta* may have had a mid-latitude preference and that the late Campanian warming at ~74 Ma (Friedrich et al., 2012) enables this species to migrate from low to mid latitudes. The latest Campanian saw a return to cooling conditions that persisted into the early Maastrichtian (Friedrich et al., 2012).
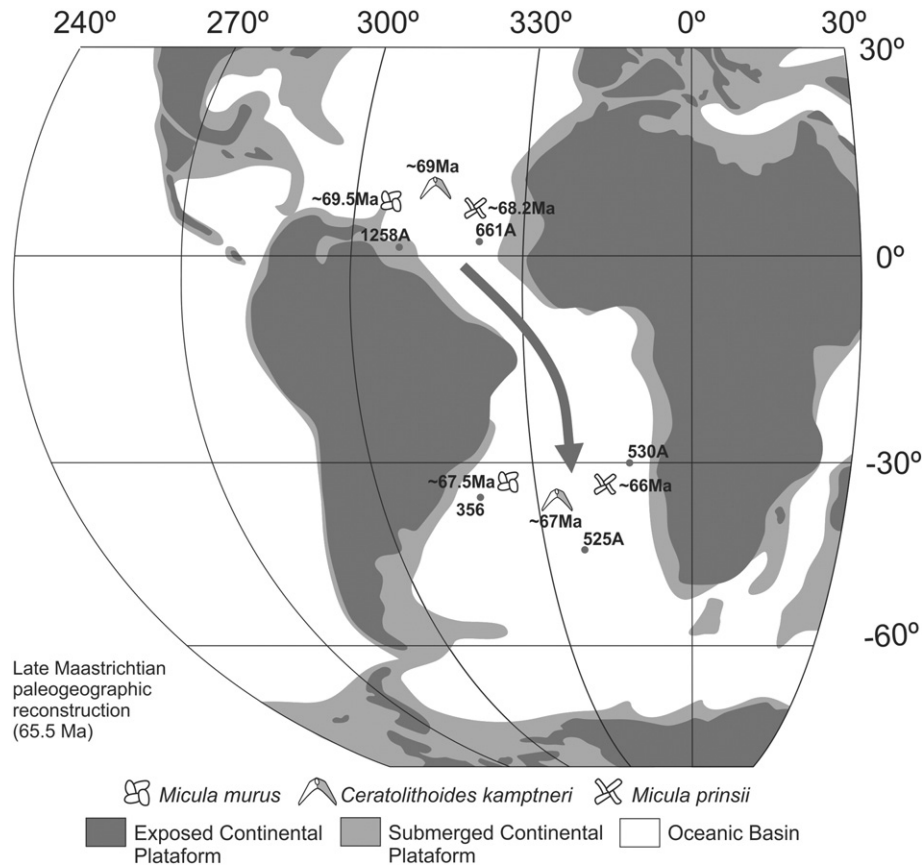
4.2.2. Maastrichtian

It appears that the LO of *R. levis* (early Maastrichtian) is a unique bio-horizon, similar in both the high and mid/low latitudes during the Maastrichtian. This bio-horizon, however, is not synchronous suggesting that a strong latitudinal ecological gradient was in place. An enhanced latitudinal temperature gradient through much of the Maastrichtian has been suggested by Linnert et al. (2014), based on temperature records from high-latitude Site 511 and the Gulf of Mexico. Thibault et al. (2010) pointed out that the planktonic foraminifera *Abathomphalus mayaroensis* has a diachronous FO from the mid latitude (Chron C31r) to the equator (top of Chron C31n; Huber and Watkins, 1992), and the nannofossil *Nephrolithus frequens* migrated from the Southern Ocean to equatorial regions within Chron C31n (Pospichal and Wise, 1990; Nifuku et al., 2008). These migrations of cool-water species can be seen as evidence of equatorial cooling during the early and early late Maastrichtian (Linnert et al., 2014), although changes in ocean circulation and evolutionary adaptations may also have had an impact (Barrera and Savin, 1999; Friedrich et al., 2009).

A striking finding of our study is that, during the late Maastrichtian (chrons C30n and C29r) most of the bio-horizons, which are evolutionary origination events, appear earlier in low latitudes and these species migrate later to the mid latitudes (Fig. 3). Thibault et al. (2010) described the latitudinal migration pattern of *M. murus* during the Maastrichtian, which supports our findings. According to those authors, this species was characteristic of warm surface waters and remained confined to the Tropical Realm during the early/late Maastrichtian before spreading out to temperate latitudes in the late Maastrichtian. Thibault et al. (2010) regarded this as suggestive of a major change in surface-water circulation, as cooler condition led to a modern style of thermohaline circulation, forced from high rather that low latitudes. Although this pattern would have impacted province boundaries and produced greater high- to low-latitude heat transport, the sequential migration of bio-horizons (FO of *M. murus*, *C. kamptneri*, *M. prinsii*) is difficult to explain, and perhaps argues against changes in ocean circulation as the predominant cause, since it would have more likely affected all species simultaneously. Although Thibault et al. (2010) argue that warmer conditions did not start until the latest Maastrichtian (Chron C29r), Friedrich et al.'s (2012) global composite record indicates that global warming may have started as early as 67 Ma (top C30n). Thus, we consider it possible that a continuous global warming trend sequentially allowed the invasion of warm-water low-latitude species at mid latitudes starting with *M. murus* (~67.5 Ma), then *C. kamptneri* (~67 Ma), and finally *M. prinsii* (~66 Ma) during the latest Maastrichtian (Fig. 5).

5. Conclusions

In this study we present new calcareous nannofossil data from nine ODP/DSDP Sites from the South Atlantic Ocean, and construct three new latitudinal-based zonations, since some bio-horizons previously considered global are found as unsuitable for biostratigraphic purposes at all

Fig. 5. Late Maastrichtian paleogeographic reconstruction (after www.odsn.de; Scotese, 2014) indicating the migration pattern of the marker species *Micula murus*, *Ceratolithoides kamptneri* and *Micula prinsii* from low to mid latitudes.

Sites. This is sometimes due to the complete absence of the marker species (e.g., *C. verbeekii* and *M. pleniporus*) and sometimes due to diachronism of bio-horizons between Sites at the same latitudinal band (e.g., *B. hayi* and *E. parallelus*). The same can be concluded for high-latitude bio-horizons, where some of the bio-horizons proposed previously were not applied because of the diachroneity (e.g., LOs of *N. corystus*, *N. watkinsii*, and *B. parca*). An important refinement was made tying the nannofossil bio-horizons to the standard magnetostratigraphic timescale (Gradstein et al., 2012).

With the use of both magnetostratigraphy and biostratigraphy, we suggest that late Campanian and late Maastrichtian species diachronism is related to migration from low to mid latitudes. The LO of *B. parca constricta* in the late Campanian occurs in Chron C32r at low latitudes later than at Chron C32n at mid latitudes, which we suggest may be related to global warming at ~74 Ma and a retraction of its range to higher latitudes. The FOs of the warm surface-water species *M. prinsii*, *C. kamptneri* and *M. murus* (Tantawy, 2003; Sheldon et al., 2010) in the late Maastrichtian occur earlier at low latitudes and these species migrate to mid latitudes sequentially during the latter part of the late Maastrichtian. This pattern may be related to ocean circulation changes and global warming that expanded the paleobiogeographic range of these species.

The proposed zones suggested herein provide a step-change in our understanding of Late Cretaceous calcareous nannofossil evolution in the South Atlantic Ocean. Due to poor recovery at some of the older sites, we envisage that future drilling in the South Atlantic will be able to build upon our findings and further constrain these zonations and paleoceanographic interpretations.

Supplementary data to this article can be found online at http://dx.doi.org/10.1016/j.palaeo.2016.04.010.

References

Antunes, R.L., 1987. Bioestratigrafia dos nanofósseis calcários Meso e Neocretáceo da porção emersa da Bacia do Espírito Santo. Bol. Geociênc. Petrobras 1 (1), 2–11.

Antunes, R.L., 1998. Nanofósseis calcários e sua bioestratigrafia no Cretáceo da Margem Continental Brasileira - Bacias do Ceará e Potiguar (Ph.D. thesis) Universidade Federal do Rio de Janeiro (193 pp.).

Barrera, E., Savin, S.M., 1999. Evolution of late Campanian–Maastrichtian marine climates and oceans. In: Barrera, E., Johnson, C.C. (Eds.), Evolution of the Cretaceous Ocean System. Geological Society of America, Special Paper Vol. 332, pp. 245–282.

Bown, P.R., Young, J.R., 1998. Techniques. In: Bown, P.R. (Ed.), Calcareous Nannofossil BiostratigraphyBritish Micropalaeontological Society Series. Chapman and Hall/Kluwer Academic Publishers, London, pp. 16–28.

Bown, P.R., Burnett, J.A., Gallagher, L.T., 1991. Critical events in the evolutionary history of calcareous nannoplankton. Hist. Biol. 5, 279–290.

Burnett, J.A., Gallagher, L.T., Hampton, M.J., 1998. Upper Cretaceous. In: Bown, P.R. (Ed.), Calcareous Nannofossil Biostratigraphy. British Micropalentological Society Series, London, pp. 132–199.

Campbell, R.J., Howe, R.W., Rexilius, J.P., 2004. Middle Campanian–lowermost Maastrichtian nannofossil and foraminiferal biostratigraphy of the northwestern Australian margin. Cretac. Res. 25, 827–864.

Clarke, L.J., Jenkyns, H.C., 1999. New oxygen isotope evidence for long-term Cretaceous climatic change in the Southern Hemisphere. Geology 27 (8), 699–702.

Concheyro, A., 2004. Mesozoic calcareous nannofossils from Larsen Basin, Southern Antarctic Peninsula. Geosur International Symposium, Buenos Aires. Extended Abstracts, pp. 255–257.

Concheyro, A., Olivera, A., Santillana, S., Marenssi, S., Rinaldi, C., 1991. Nanofósiles calcáreos del Cretácico Superior de Isla Marambio, Antártida. Congreso Geologico Chileno. Resúmenes Expandidos, pp. 825–828.

Concheyro, A., Robles Hurtado, G.M., Olivero, E.B., 1994. Micropaleontologia del Nunatak Sanctuary Cliffs, Isla Snow Hill y de Cabo Hamilton, Isla James Ross, Antartida. Terceras Jornadas de Comunicaciones sobre investigaciones Antárticas, Buenos Aires. Resúmenes, pp. 17–23.

Crux, J.A., 1991. Calcareous nannofossils recovered by Leg 114 in the Subantarctic South Atlantic Ocean. In: Ciesielski, P.F., Kristoffersen, Y., et al. (Eds.), Proceedings of the Ocean Drilling Program. Scientific Results Vol. 114, pp. 155–177.

Erba, E., 1992. Middle Cretaceous calcareous nannofossils from the western Pacific (LEG 129): evidence for paleoequatorial crossings. In: Larson, R.L., Lancelot, Y., et al. (Eds.), Proceedings of the Ocean Drilling Program. Scientific Results Vol. 129, pp. 189–201.

Erba, E., 2004. Calcareous nannofossils and Mesozoic oceanic anoxic events. Mar. Micropaleontol. 52, 85–106.

Erbacher, J., Mosher, D.C., Malone, M.J., Berti, D., Bice, K.L., Bostock, H., Brumsack, H.-J., Danelian, T., Forster, A., Glatz, C., Heidersdorf, F., Henderiks, J., Janecek, T.R., Junium, C., Le Callonnec, L., MacLeod, K., Meyers, P.A., Mutterlose, H.J., Nishi, H., Norris, R.D., Ogg, J.G., O'Regan, A.M., Rea, B., Sexton, P., Sturt, H., Suganuma, Y., Thurow, J.W., Wilson, P.A., Wise, S.W., 2004. Site 1258. In: Erbacher, J., Mosher, D.C., Malone, M.J., et al. (Eds.), Proceedings of the Ocean Drilling Program. Initial Reports vol. 207 (117 pp.).

Forster, A., Schouten, S., Baas, M., Damsté, J.S.S., 2007. Mid-Cretaceous (Albian-Santonian) sea surface temperature record of the tropical Atlantic Ocean. Geology 35, 919–922.

Freitas, L.C.S., 1984. Nanofósseis calcários e sua distribuição (Aptiano-Mioceno) na Bacia Sergipe-Alagoas (Master dissertation) Universidade Federal do Rio de Janeiro (247 pp.).

Friedrich, O., Herrle, J.O., Wilson, P.A., Cooper, M.J., Erbacher, J., Hemleben, C., 2009. The early Maastrichtian carbone cycle perturbation and cooling event: implications from the South Atlantic Ocean. Paleoceanography 24, PA2211. http://dx.doi.org/10.1029/2008PA001654.

Friedrich, O., Norris, R.D., Erbacher, J., 2012. Evolution of middle to Late Cretaceous oceans — a 55 m.y. record of Earth's temperature and carbon cycle. Geology 40, 107–110.

Gardin, S., Galbrun, B., Thibault, N., Coccioni, R., Premoli-Silva, I., 2012. Biomagnetocronology for the upper Campanian–Maastrichtian from the Gubbio area, Italy: new results from the Contessa Highway and Bottaccione sections. Newsl. Stratigr. 45 (1), 75–103.

Gomide, J., 1989. Bacia de Pelotas: Biocronoestratigrafia baseada em nanofósseis calcários. Congresso brasileiro de Paleontologia Vol. 11. SBP, Anais, Curitiba, pp. 338–351.

Gradstein, F.M., Ogg, J.G., Schmitz, M.D., Ogg, G.M., 2012. The Geologic Time Scale 2012. Elsevier, Amsterdam (2 vols.).

Guerra, R.M., Tokutake, L.R., Fauth, G., 2010. Upper Campanian calcareous nannofossils from a core of well 2-RSS-1, Pelotas Basin, Brazil. Rev. Bras. Paleontol. 13 (3), 181–188.

Guerra, R.M., Concheyro, A., Lees, J., Fauth, G., Carvalho, M.A., Ramos, R.R.C., 2015. Calcareous nannofossils from the Santa Marta Formation (Upper Cretaceous), northern James Ross Island, Antarctic Peninsula. Cretac. Res. 56, 550–562.

Guerra, R.M., Tokutake, L.R., Fauth, G., 2012. Cretaceous calcareous nannofossils from Pelotas Basin, Brazil: biostratigraphic and paleoecological inferences. J. S. Am. Earth Sci. 36, 55–71.

Hailwood, E.A., Clement, B.M., 1991. Magnetostratigraphy of Sites 699 and 700, East Georgia Basin. In: Ciesielski, P.F., Kristoffersen, Y., et al. (Eds.), Proceedings of the Ocean Drilling Program. Scientific Results Vol. 114, pp. 337–358.

Hamilton, N., 1990. Mesozoic magnetostratigraphy of Maud Rise, Antarctica. In: Barker, P.F., Kennett, J.P., et al. (Eds.), Proceedings of the Ocean Drilling Program. Scientific Results Vol. 113, pp. 255–260.

Hardas, P., Mutterlose, J., Friedrich, O., Erbacher, J., 2012. The Middle Cenomanian Event in the equatorial Atlantic: the calcareous nannofossil and benthic foraminiferal response. Mar. Micropaleontol. 96-97, 66–74.

Howe, R.W., Campbell, R.J., Rexilius, J., 2003. Integrated uppermost Campanian–Maastrichtian calcareous nannofossil and foraminiferal biostratigraphic zonation of the northwestern margin of Australia. J. Micropalaeontol. 22, 29–62.

Huber, B.T., Watkins, D.K., 1992. Biogeography of Campanian-Maastrichtian calcareous plankton in the region of the Southern Ocean: paleogeographic and paleoclimatic implications. Am. Geophy. Union, Antarctic Research Series 56, 31–60.

Huber, B.T., Hodell, D.A., Hamilton, C.P., 1995. Middle–Late Cretaceous climate of the southern high latitudes: stable isotopic evidence for minimal equator-to-pole thermal gradients. Bull. Geol. Soc. Am. 107, 1164–1191.

Huber, B.T., Norris, R.D., MacLeod, K.G., 2002. Deep-sea paleotemperature record of extreme warmth during the Cretaceous. Geology 30 (2), 123–126.

Jenkyns, H.C., Gale, A.S., Corfield, R.M., 1994. Carbon- and oxygen-isotope stratigraphy of the English Chalk and Italian Scaglia and its palaeoclimatic significance. Geol. Mag. 131, 1–34.

Keating, B.H., Herrero-Bervera, E., 1985. Magnetostratigraphy of Cretaceous and Early Cenozoic sediments of Deep Sea Drilling Project Site 530, Angola Basin. In: Hay, W.W., Sibuet, J.C., et al. (Eds.), Initial Reports of the DSDP Vol. 75, pp. 1211–1218.

Lees, J.A., 2002. Calcareous nannofossil biogeography illustrates palaeoclimate change in the Late Cretaceous Indian Ocean. Cretac. Res. 23, 537–634.

Lees, J.A., Bown, P.R., 2005. Upper Cretaceous calcareous nannofossil biostratigraphy, ODP Leg 198 (Shatsky Rise, Northwest Pacific Ocean). In: Bralower, T.J., Premoli Silva, I., Malone, M.J. (Eds.), Proceedings of the Ocean Drilling Program. Scientific Results Vol. 198, pp. 1–60.

Lees, J.A., Bown, P.R., Mattioli, E., 2005. Problem with proxies? Cautionary tales of calcareous nannofossil paleoenvironmental indicators. Micropaleontology 51 (4), 333–343.

Li, L., Keller, G., 1998. Abrupt deep-sea warming at the end ofthe Cretaceous. Geology 26, 995–998.

Linnert, C., Mutterlose, J., 2015. Boreal early Turonian calcareous nannofossils from nearshore settings — implications for Paleoecology. PALAIOS 30, 728–742.

Linnert, C., Robinson, S.A., Lees, J.A., Bown, P.R., Pérez-Rodríguez, I., Petrizzo, M.R., Falzoni, F., Littler, K., Arz, J.A., Russell, E.E., 2014. Evidence for global cooling in the Late Cretaceous. Nat. Commun. 5 (4194), 1–7.

Manivit, H., 1984. Paleogene and Upper Cretaceous calcareous nannofossils from Deep Sea Drilling Project Leg 74. In: Moore, T.C., Rabinowitz, P.D., et al. (Eds.), Initial Reports of the DSDP Vol. 74, pp. 475–499.

Manivit, H., 1989. Calcareous nannofossil biostratigraphy of Leg 108 sediments. In: Ruddiman, W., Sarnthein, M., et al. (Eds.), Proceedings of the Ocean Drilling Program. Scientific Results Vol. 108, pp. 35–69.

Manivit, H., Feinberg, H., 1984. Correlation of magnetostratigraphy and nannofossil biostratigraphy in Upper Cretaceous and Lower Paleocene sediments of the Walvis Ridge area. In: Moore, T.C., Rabinowitz, P.D., et al. (Eds.), Initial Reports of the DSDP Vol. 74, pp. 469–474.

Mutterlose, J., Bornemann, A., Herrle, J.O., 2005. Mesozoic calcareous nannofossils — state of the art. Paläontol. Z. 79, 113–133.

Nifuku, K., Kodama, K., Shigeta, Y., Naruse, H., 2008. Faunal turnover at the end of the Cretaceous in the North Pacific region: implications from combined magnetostratigraphy and biostratigraphy of the Maastrichtian Senpohshi Formation in the eastern Hokkaido Island, northern Japan. Palaeogeogr. Palaeoclimatol. Palaeoecol. 271, 84–95.

Oliveira, L.C.V., 1997. Arcabouço estratigráfico Albo-Maastrichtiano da Bacia de Campos: um estudo com base em nanofósseis calcáreos e suas correlações com marcos elétricos e a estratigrafia química (Master dissertation) Universidade Federal do Rio Grande do Sul (180 pp.).

Oliveira, L.C.V., Costa, S.O., 1997. Proposal of new biostratigraphic units based on calcareous nannofossils for the Maastrichtian of the Santos Basin (Brazil). An. Acad. Bras. Cienc. 69 (1), 37–58.

Perch-Nielsen, K., 1977. Albian to Pleistocene calcareous nannofossils from the Western South Atlantic, DSDP Leg 39. In: Supko, P.R., Perch-Nielsen, K., et al. (Eds.), Initial Reports of the DSDP Vol. 39, pp. 699–823.

Perch-Nielsen, K., 1985. Mesozoic calcareous nannofossils. In: Bolli, H.M., Saunders, J.B., Perch-Nielsen, K. (Eds.), Plankton Stratigraphy Vol. 1. Cambridge University Press, Cambridge, pp. 329–426.

Pérez-Rodríguez, I., Lees, J.A., Larrasoaña, J.C., Arz, J.A., Arenillas, I., 2012. Planktonic foraminiferal and calcareous nannofossil biostratigraphy and magnetostratigraphy of the uppermost Campanian and Maastrichtian at Zumaia, northern Spain. Cretac. Res. 37, 100–131.

Pospichal, J.J., Wise, S.W., 1990. Maestrichtian calcareous nannofossil biostratigraphy of Maud Rise, ODP Leg 113 Sites 689 and 690, Weddell Sea. In: Barker, P.F., Kennett, J.P., et al. (Eds.), Proceedings of the Ocean Drilling Program. Scientific Results Vol. 113, pp. 465–487.

Roth, P.H., 1983. Jurassic and Lower Cretaceous calcareous nannofossils in the Western North Atlantic (Site 534): biostratigraphy, preservation, and some observations on biogeography and paleoceanography. In: Sheridan, R.E., Gradstein, F.M., et al. (Eds.), Initial Reports of the DSDP Vol. 76, pp. 587–621.

Roth, P.H., Krumbach, K.R., 1986. Middle Cretaceous calcareous nannofossil biogeography and preservation in the Atlantic and Indian Oceans: implications for palaeoceanography. Mar. Micropaleontol. 10, 235–266.

Roth, P.H., Thierstein, H., 1972. Calcareous nannoplankton: Leg 14 of the Deep Sea Drilling Project. In: Hayes, D.E., Pimm, A.C., et al. (Eds.), Initial Reports of the DSDP Vol. 14, pp. 421–485.

Scotese, C.R., 2014. Atlas of Late Cretaceous Maps. PALEOMAP Atlas for ArcGis, Volume 2, the Cretaceous, Maps 16–22, Mollweide Projection. PALEOMAP Project, Evanston, IL.

Self-Trail, J.M., 2001. Biostratigraphic subdivision and correlation of upper Maastrichtian sediments from the Atlantic Coastal Plain and Blake Nose, western Atlantic. In: Kroon, D., Norris, R.D., Klaus, A. (Eds.), Western North Atlantic Palaeogene and Cretaceous Palaeoceanography. Geological Society, London, Special Publications Vol. 183, pp. 93–110.

Shafik, S., 1990. Late Cretaceous nannofossil biostratigraphy and biogeography of the Australian western margin. Bur. Mineral. Resour. Geol. Geophys. Rep. 295, 1–164.

Sheldon, E., 2008. Upper Campanian–Maastrichtian calcareous nannofossil biostratigraphy of the Stevns-1 borehole, Denmark. J. Nannoplankton Res. 30 (1), 39–49.

Sheldon, E., Ineson, J., Bown, P.R., 2010. Late Maastrichtian warming in the Boreal Realm: Calcareous nannofossil evidence from Denmark. Palaeogeogr. Palaeoclimatol. Palaeoecol. 295, 55–75.

Stradner, H., Steinmetz, J., 1984. Cretaceous calcareous nannofossils from the Angola Basin, Deep Sea Drilling Project Site 530. In: Hay, W.W., Sibuet, J.-C., et al. (Eds.), Initial Reports of the DSDP Vol. 75, pp. 565–649.

Švábenická, L., Vodrážka, R., Nývlt, D., 2012. Calcareous nannofossils from the Upper Cretaceous of northern James Ross Island, Antarctica: a pilot study. Geol. Q. 56 (4), 765–772.

Tantawy, A.A.A.M., 2003. Calcareous nannofossil biostratigraphy and paleoecology of the Cretaceous-Tertiary transition in the central eastern desert of Egypt. Mar. Micropaleontol. 47, 323–356.

Thibault, N., Gardin, S., 2006. Maastrichtian calcareous nannofossil biostratigraphy and paleoecology in the Equatorial Atlantic (Demerara Rise, ODP Leg 207 Hole 1258A). Rev. Micropaleontol. 49, 199–214.

Thibault, N., Gardin, S., 2007. The Late Maastrichtian nannofossil record of climate change in the South Atlantic DSDP Hole 525 A. Mar. Micropaleontol. 65, 163–184.

Thibault, N., Husson, D., 2016. Climatic fluctuations and sea surface water circulation patterns at the end of the Cretaceous era: calcareous nannofossil evidence. Palaeogeogr. Palaeoclimatol. Palaeoecol. 441 (1), 152–164.

Thibault, N., Gardin, S., Galbrun, B., 2010. Latitudinal migration of calcareous nannofossil *Micula murus* in the Maastrichtian: implications for global climate change. Geology 38 (3), 203–206.

Thibault, N., Husson, D., Harlou, R., Gardin, S., Galbrun, B., Huret, E., Minoletti, F., 2012. Astronomical calibration of upper Campanian–Maastrichtian carbon isotope events and calcareous plankton biostratigraphy in the Indian Ocean (ODP Hole 762C): implication for the age of the Campanian–Maastrichtian boundary. Palaeogeogr. Palaeoclimatol. Palaeoecol. 337-338, 52–71.

Thierstein, H.R., 1981. Late Cretaceous nannoplankton and the change at the Cretaceous–Tertiary boundary. SEPM Spec. Publ. 32, 355–394.

Troelsen, J.C., Quadros, L.P., 1971. Distribuição bioestratigráfica dos nanofósseis em sedimentos marinhos (Aptiano-Mioceno) do Brasil. An. Acad. Bras. Geociênc. 43 (suplemento), 577–609.

Watkins, D.K., 1989. Nannoplankton productivity fluctuations and rhythmically bedded pelagic carbonates of the Greenhorn Limestone (Upper Cretaceous). Palaeogeogr. Palaeoclimatol. Palaeoecol. 74, 75–86.

Watkins, D.K., Self-Trail, J.M., 2005. Calcareous nannofossil evidence for the existence of the Gulf Stream during the Maastrichtian. Paleoceanography 20, PA3006. http://dx.doi.org/10.1029/2004PA001121.

Watkins, D.K., Wise, S.W., Pospichal, J.J., Crux, J., 1996. Upper Cretaceous calcareous nannofossil biostratigraphy and paleoceanography of the Southern Ocean. In:

Moguilevsky, A., Whatley, R. (Eds.), Microfossils and Oceanic Environments. University of Wales, Aberystwyth Press, pp. 355–381.

Wind, F.H., 1979. Maestrichtian–Campanian nannofloral provinces of the southern Atlantic and Indian oceans. In: Talwani, M., Hay, W., Ryan, W.B.F. (Eds.), Deep Sea Drilling Results in the Atlantic Ocean: Continental Margins and Paleoenvironment, pp. 123–137.

Wind, F.H., Wise, S.W., 1983. Correlation of Upper Campanian–Lower Maastrichtian calcareous nannofossil assemblages in drill and piston cores from the Falkland Plateau, Southwest Atlantic Ocean. In: Ludwig, W.J., Krasheninnikov, V.A., et al. (Eds.), Initial Reports of the DSDP Vol. 71, pp. 551–563.

Winter, A., Jordan, R., Roth, P.H., 1994. Biogeography of living coccolithophores in ocean waters. In: Winter, A., Siesser, W.G. (Eds.), Coccolithophores. Cambridge University Press, Cambridge, pp. 161–177.

Wise, S.W., 1983. Mesozoic and Cenozoic calcareous nannofossils recovered by Deep Sea Drilling Project Leg 71 in the Falkland Plateau Region, Southwest Atlantic Ocean. In: Ludwig, W.J., Krasheninnikov, V.A., et al. (Eds.), Initial Reports of the DSDP Vol. 71, pp. 481–550.

Wise, S.W., 1988. Mesozoic–Cenozoic history of calcareous nannofossils in the region of the Southern Ocean. Palaeogeogr. Palaeoclimatol. Palaeoecol. 67, 157–179.

Wise, S.W., Wind, F.H., 1977. Mesozoic and Cenozoic calcareous nannofossils recovered by DSDP Leg 36 Drilling on the Falkland Plateau, Southwest Atlantic Sector of the Southern Ocean. In: Barker, P.F., Dalziel, I.W.D., et al. (Eds.), Initial Reports of the DSDP Vol. 36, pp. 269–491.

Young, J.R., Bown, P.R., Lees, J.A., (Eds.) Nannotax3 Website. International Nannoplankton Association. (URL: http://ina.tmsoc.org/Nannotax3).

Ziveri, P., Baumann, K.-H., Bökel, B., Bollmann, J., Young, J.R., 2004. Biogeography of selected Holocene coccoliths in the Atlantic Ocean. In: H.R., Thierstein., Young, J.R. (Eds.), Coccolithophores: From Molecular Process to Global Impact. Springer Verlag, Berlin, Germany, pp. 403–428.